Proceedings of the ASME 2010 International Mechanical Engineering Congress & Exposition
IMECE2010
November 12-18, 2010, Vancouver, British Columbia, Canada

IMECE2010-40517

MICROFLOW CYTOMETER: HYDRODYNAMIC FOCUSING AND SEPARATION OF SAMPLE STREAM

Nastaran Hashemi,
Center for Bio/Molecular Science and Engineering
Naval Research Laboratory
Washington, DC, USA
nastaran.hashemi.ctr@nrl.navy.mil

Peter B. Howell, Jr.,
Center for Bio/Molecular Science and Engineering
Naval Research Laboratory
Washington, DC, USA
peter.howell@nrl.navy.mil

Frances S. Ligler
Center for Bio/Molecular Science and Engineering
Naval Research Laboratory
Washington, DC, USA
fran.ligler@nrl.navy.mil

ABSTRACT
Using grooves in the walls of a microchannel and two sheath streams, we have passively focused a sample stream in the center of the microchannel for optical analysis. Even though the sample stream is completely surrounded by sheath fluid, reversing the orientation of the grooves in the channel walls returns the sample stream to its original position with respect to the sheath streams. The use of this sheathing technique has already been demonstrated in a sensitive microflow cytometer; the unsheathing capability now provides the opportunity to recover particles from the sensor with minimal dilution or to recycle the sheath fluid for long-term unattended operation. The ability to reverse focused laminar flows opens a variety of options for combining target transport, processing and analysis procedures.

INTRODUCTION
Flow cytometry is used to count and characterize cells and particles. In the traditional design, the sample stream exiting a small channel is introduced into the center of a larger channel containing sheath fluid. Then the larger channel constricts to force the cells or particles to travel in single file along a fixed and precise trajectory within the flow channel. Since the cells are following the same path, they all have the same velocity and can be interrogated with low variance.

Over the last decades, researchers in the microfluidics community have focused on using microfluidics to create microflow cytometers with very small footprints. Furthermore, hydrodynamic focusing of one laminar stream by another without mixing has inspired new approaches for separations, optical components, biosensors, and cell analysis.[3,5,6,7,8,9] Creating sheathed flow by placing a small tube inside a larger one is hard to microfabricate. Jacobson and Ramsey used a cross intersection to create sheathed flow. [10] Later on, Blankenstein and Larsen used pressure-driven flow for the interrogation of polystyrene beads for cytometry. [11] Howell et al. presented two designs that can create fully sheathed flow in a microdevice.

In the first design, a T-junction directed the sample and sheath streams side-by-side into the channel. A set of straight diagonal grooves on the top and bottom of the channel wrapped the sample fluid with sheath fluid. Passing through more grooves, the sheath fluid moved toward the far side of the sample stream and sample stream became focused more toward the center of the channel. Fig. 1A shows numerical simulation of this design using Tiny-3D.[23] The chips were made in polymethyl methacrylate (PMMA) using a Haas Minimill to experimentally demonstrate the sheathing process. Channel dimensions were 450 µm wide by 150 µm deep. The grooves were 150 µm wide by 75 µm deep at 45◦ relative to the axis of the channel. Fig. 1B shows the dye-labeled sample stream is brought to the center of the channel by 5 pairs of stripes.

In the other design, shown in Fig. 2, the sheath solution was divided equally between the two inlets of a T-intersection to position the sample stream in the center of the channel. A set of chevrons cut into the top and

bottom of the channel transferred sheath fluid from the sides to the middle along the top and bottom, and compressed the sample stream vertically. The sample could be more compressed by adding more chevrons. The chevrons placed the sample stream in the center of the channel regardless of the flow ratios as opposed to the straight-groove design. In this design, the number of chevrons controlled the height of the sample and the flow ratio controlled the width.

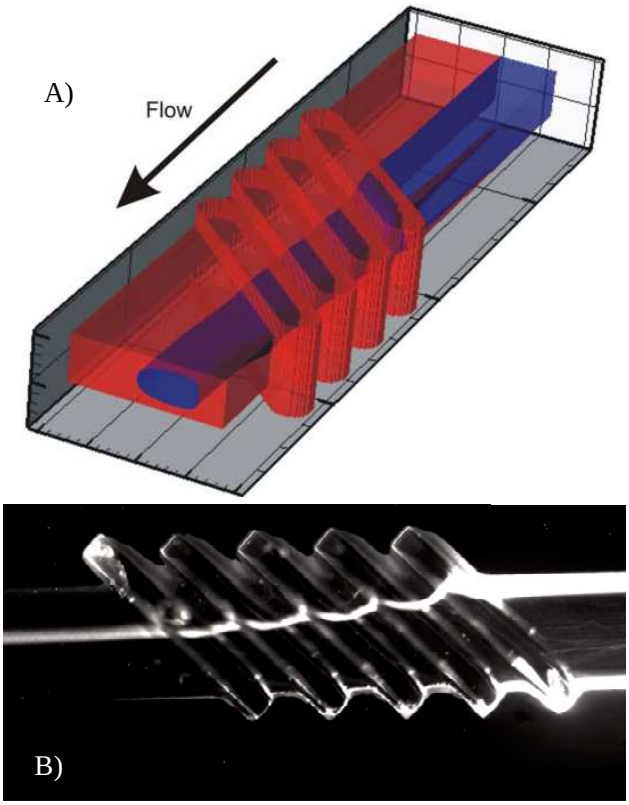

Fig. 1: (A) Numerical simulation of sheathing the sample stream (blue) by the sheath solution (red). (B) The sample stream has been labeled with a rhodamine dye and it is seen by its fluorescence [24].

The microchannels were manufactured in polydimethylsiloxane (PDMS) using standard soft lithography procedures.[18] Fluidic inlets were cored into the top of the PDMS module. Silicone tubing with an internal diameter of 760 μm connected to the inlets. Channel dimensions were 390 μm wide by 130 μm deep. The chevron-shaped grooves were 100 μm wide by 65 μm deep and intersected the channel wall at 45 degrees.

Control of flow streams using grooves has recently been used to develop very sensitive microflow cytometers.[9,25] This hydrodynamic positioning, along with control of the relative flow rates of the sheath and sample streams, focused the sample stream as it crossed the laser beams in the interrogation region to generate three-color fluorescence and light scatter signals. The data obtained in a six-target assay using the microflow cytometer were equivalent to data obtained using a commercial benchtop cytometer.[25] No mixing occurred between the sheath and sample streams.

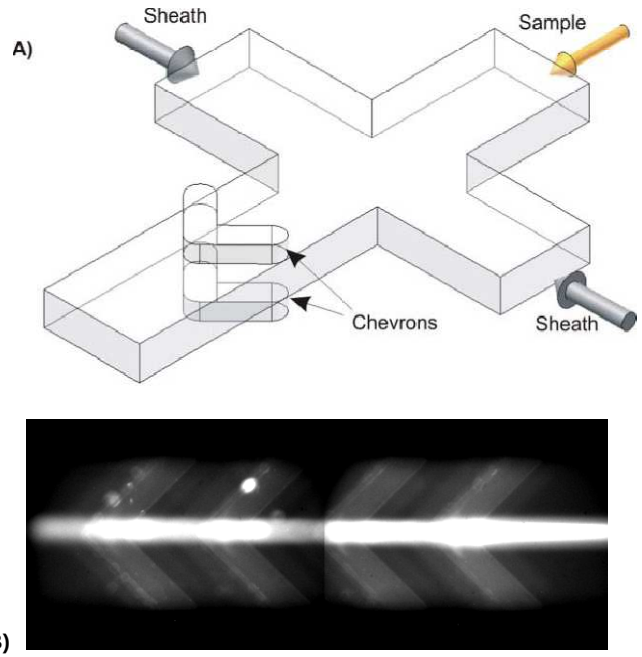

Fig. 2: (A) Schematic of the inlet and a chevron for the chevron-based sheath flow design. (B) Microscopy image of the PDMS channel. The sample stream includes a fluorescent dye.

Mixing limitations at low Reynolds numbers have been another area of microfluidics that have received a great deal of attention.[1,2,4] To design efficient microfluidic mixers, Howell *et al.* used a Navier-Stokes solver (NSS) to create three-dimensional flow field.[22] The channel cross-section at the inlet was divided into a 22x64 grid of cells and 5 points were chosen for each cell. Using a full NSS and Lagrangian advection routine, the lateral and horizontal displacement of a particle at each point was found. In experiments, it was found that for $0 < Re < 150$ the outflow plane created by a specific mixer was independent of Re. Increasing Re above150, the outflow plane began to differ from what predicted by the numerical solver. This was due to inertial effects which caused changes in the behavior of the systems. It was also found that the effect a feature had on the distribution within the channel was reversible. This was due to the operation of the mixers in the Stokes flow regime. Fig. 3 shows a set of feature pairs which have no net effect on the flow. In general any set of features that contained a mirror plane normal to the channel would have no net effect on the bulk flow within the channel. Any operation performed by the feature upstream of the mirror plane would be negated by the downstream feature.

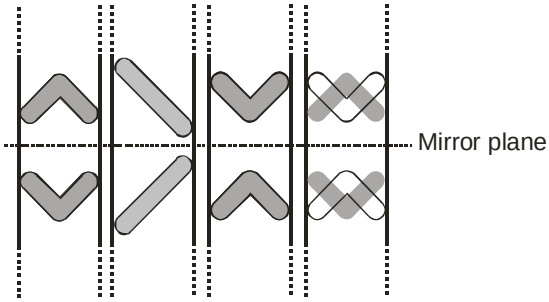

Fig. 3: In mixer designs, these feature pairs have no effect on the flow due to symmetry [22].

In the Stokes flow regime, repeating a given mixer design did not necessarily improve ultimate degree of mixing. Fig. 4 shows the reversibility of the mixing in a particular mixer design. A combination of 10 features of straight and chevron grooves was used to mix the two streams, then a longitudinal reflection of the same 10 features was used to unmix them. Most of the dye was returned to the left side of the channel. We contributed the imperfect unmixing to the irregularities in machining the channel.

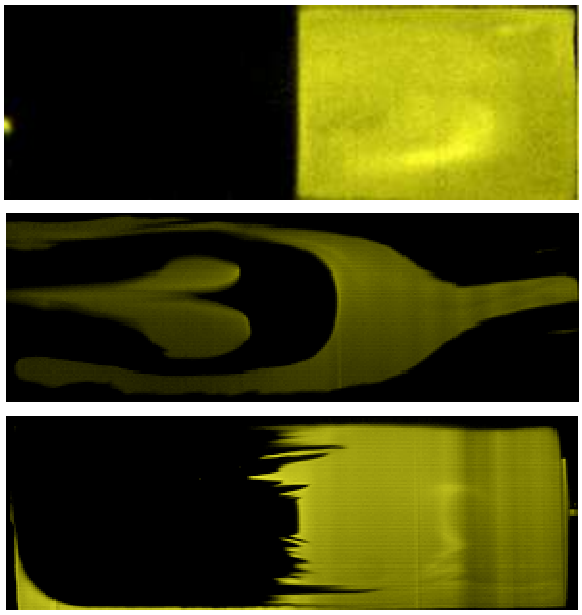

Fig. 4: Reversibility of geometric mixing. Top figure shows the mixing after the mixing and the bottom figure show the cross section after unmixing [19].

While symmetrical features are not desirable in mixing, they can be used to unmix and separate a flow stream from another. At low Reynolds number, the dynamics of fluids can be reversed by reversing the direction of the forces applied to the system.[14,15,16,17,18,19] In microfluidic devices, flows are mainly dominated by viscosity, and inertia plays a marginal role. The equations of motion in viscosity-dominated flows are linear and do not depend explicitly on time. In his classic video clip, Taylor [16] demonstrated that a drop of dye added to a viscous fluid between two cylinders could be stretched by rotating the outer cylinder and reconstituted by reversing the direction of rotation. Heller also demonstrated unmixing by reversal of motion while observing thermal agitation of molecules.[20] Fuerstman *et al.* [14] investigated reversibility to encrypt and decrypt information. Sundararajan et al. investigated the reversibility of convection-diffusion in laminar chaotic flows in a patterned microchannel.[5]

RESULTS AND DISCUSSIONS

Using the reversibility in the laminar flow regime, we designed a microdevice that returns the sample stream to its original position with respect to the sheath streams. We have shown both in simulation and experimentally that the sample stream could be ensheathed, focused, and separated from the sheath streams.[12] A microdevice including four grooves used for sheathing and four reversed grooves used for unsheathing was designed (Fig. 5).

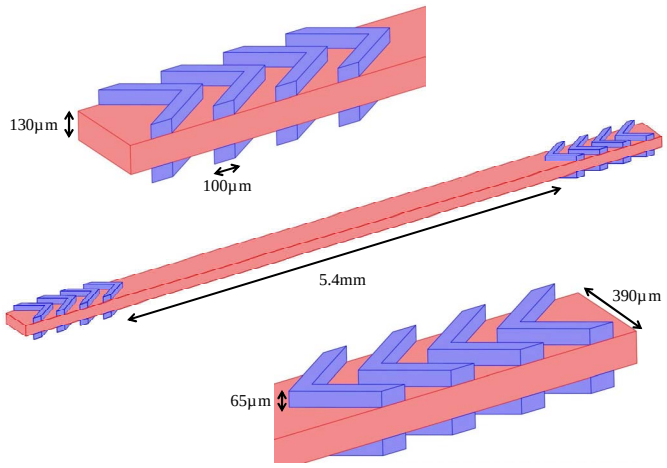

Fig. 5: Schematic of the microchannel. The distance between the sheathing and unsheathing chevron structures is 5.4 mm [12].

A flow channel was created using soft lithography.[26] Sheath flow was introduced on both sides of the sample stream using a bifurcated tube extending from a single reservoir (Fig. 6A). The chevron-shaped grooves performed the sheathing by moving some of the sheath fluid to above and below the sample stream. To reverse the sheathing, a second set of chevron-shaped grooves was placed in the channel pointing upstream, i.e. symmetrical to the first set with an axis of symmetry across the middle of the channel as shown in Fig. 6B. A single pump pulled the sheath fluid out of the channel from both sides, recirculating it back into the channel on

both sides of the sample inlet. In order to vary the volume of sheath fluid recycled, relative to the volume of sheath fluid introduced, pumps were placed at both the center inlet and center outlet. Increasing the flow rate of the exit pump relative to the inlet pump caused sheath fluid as well as sample fluid to be removed from recirculation.

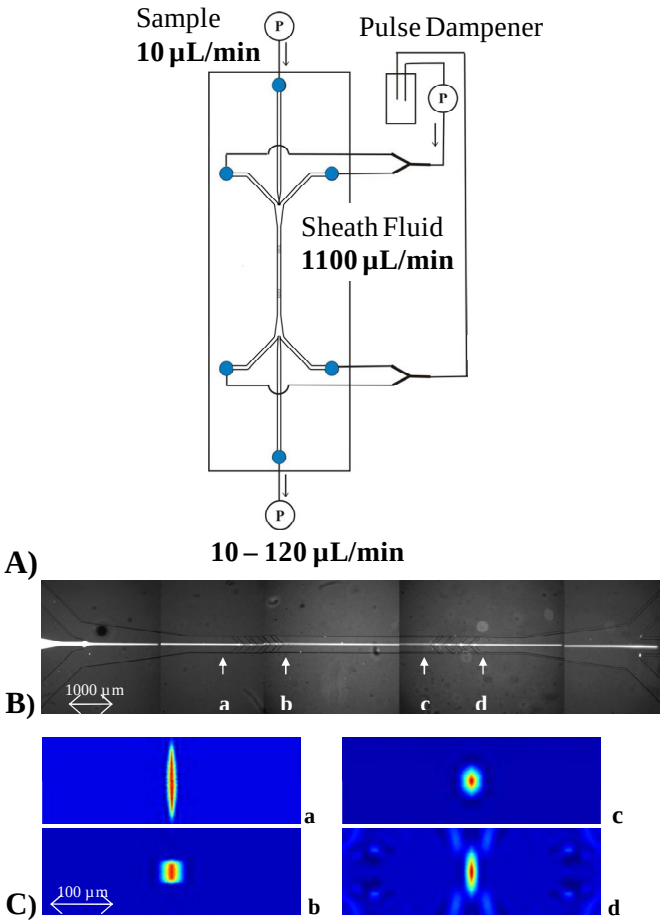

Fig. 6: (A) Schematic of experimental setup. (B) The image of the microfluidic channel shows the fluorescent sample fluid entering the channel between the two sheath inlets and exiting between the two sheath outlets. Note that the fluorescence appears dimmer between the chevrons where the sample stream does not reach the top of the channel. (C) Simulation showing concentration distribution for low molecular weight components in the sample steam (e.g. dye) at a sheath (blue) and sample (red) flow rates of 1000 and 10 µL/min, respectively. The cross sections in the simulation were selected at positions that correspond to the locations in the actual microchannel as marked in the micrograph: a) before inlet chevrons, b) after inlet chevrons, c) before reverse chevrons, and d) after reverse chevrons.

The simulation in Fig. 6C represents the positions of the sheath and sample streams at different cross sections throughout the channel at a sheath flow rate of 1100 µL/min and a sample flow rate of 10 µL/min. Diffusive transport calculations indicate the diffusion of low molecular weight molecules from the sample into the sheath stream. Navier-Stokes equations for incompressible flow at steady state were used to numerically solve for the continuity and the momentum balance.

$$(\mathbf{u}\ .\nabla)\mathbf{u} = -\frac{1}{\rho}\nabla p + \nu\nabla^2\mathbf{u}$$
$$\nabla .\ \mathbf{u} = 0 \qquad \text{Eq. 1}$$

Here ρ represents density, **u** is the velocity vector, p is the pressure, and ν is the kinematic viscosity. Since the inertial forces are negligible at low Reynolds number, the motion of the fluid can be approximately described by the reversible Stokes equation in which the nonlinear term can be neglected.[14, 27] To describe the diffusive transport in the microchannel Fick's law was used.

$$-\nabla .(-D\,\nabla c + c\mathbf{u}) = 0 \qquad \text{Eq. 2}$$

D is the diffusion coefficient and c represents the concentration. Assuming that a change in concentration does not affect the viscosity and density of the fluid, the Navier-Stokes equations were solved first and followed by the convection-diffusion relationships.

The sample stream was completely surrounded by the sheath stream after passing the first set of chevrons. At the flow rates utilized, diffusion was limited as the sample stream passed down the channel. After passing through the reverse chevrons, the sample stream returned most of the way to the top and bottom of the channel, with diffusion preventing a complete return to the narrow stream width exhibited at the entrance. Confocal microscopy verified that the stream was pushed away from the top of the channel between the chevrons and returned to a position near the channel top after the reversed chevrons. The micrographs also verify that the sample stream remained centered in the channel without significant mixing or diffusion (Fig. 7).

To confirm the reversibility experimentally, we included a low molecular weight fluorescent dye and 5µm polystyrene beads (400 beads/µL) in the sample stream. The hydrophobicity of the beads caused some loss due to sticking in the inlet tubing. We collected 1 mL of the sample drawn from the sample outlet channel and measured the recovery of the fluorescent dye and beads as they exited the center outlet channel (Fig. 8).

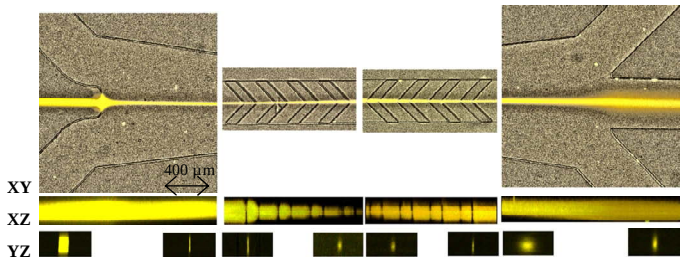

Fig. 7: Confocal microscopy images of the sheathing and unsheathing processes at 90% sheath fluid recycling. XY: Top view of the inlet, inlet chevrons, reverse chevrons, and outlet sections of the microchannel. XZ: Side view of the same sections. YZ: Cross section view at upstream and downstream side of each section. The sample height decreases upon passing through the inlet chevrons and increases by passing through each reverse chevron. The sample flow rate is 10 µL/min and the sheath flow rate is 1100 µL/min.[12]

The concentration of fluorescent dye exiting the center outlet channel was quantified using a full-spectrum UV/Vis spectrophotometer and was compared to the dye concentration entering the center inlet. To count the polystyrene beads, we used an Accuri flow cytometer. The numbers of beads exiting the center channel was reported directly; at 90% sheath recycling, no beads were detected in the recycled sheath fluid. We found that as the proportion of fluid drawn out of the center of the microchannel increased, the recovery of the fluorescence and beads increased. Since the system was a closed loop, drawing the sample stream with faster flow rate resulted in a drop in volume of sheath fluid recycled. All of the fluorescent dye, and thus 100% of the sample stream, was recovered when the system was operated with 90% sheath recycling. The maximum numbers of beads were recaptured at sheath recycling levels $\leq$92%. Our results confirm that at high Peclet numbers or low Reynolds numbers, small particles follow the fluid streamlines and travel along the average fluid flow direction.[28]

CONCLUSION

The reversibility of the hydrodynamic focusing has application for automated processing of cells and particles, for long-term unattended use of flow cytometers, and for improved cell recovery after sorting of tumor and stem cells. For example, cells could be mixed with more rapidly diffusing dyes and then recaptured in their original volume. Cytometers with recycled sheath fluid could be used to monitor recycled drinking water for bacterial contamination on the space shuttle or to reduce the size and logistical burden of systems that monitor the air for release of biothreat agents.[29] Finally, circulating tumor cells could be concentrated for culture or PCR after identification by flow cytometery without immunomagnetic separation or centrifugation.[30]

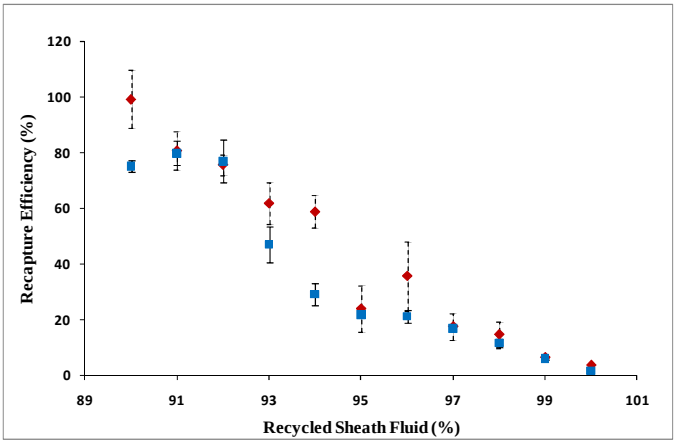

Fig. 8: (◊) The percentage of the fluorescent dye recaptured increased as the proportion of sheath fluid recycled decreased. (□) The recovery of the 5 micron microspheres, compared to the 400/µL recoverable at 83% sheath recycling, was maximized at $\leq$92% sheath recycling. Values in both graphs are the mean and standard deviation from 4 experiments; in some cases the standard deviations are small enough for the bars to be obscured by the markers for the mean.

ACKNOWLEDGMENTS

NH is an ASEE Postdoctoral Fellow. This work was supported by NIH Partnership Grant 1UO1AI075489 and NRL 6.2 work unit 69-6339. The views are the authors own and do not represent opinion or policy of NIH, HHS, the US Navy or DoD.

REFERENCES

1. A.D. Stroock, S.K.W. Dertinger, A.Ajdari, I. Mezic, H. A. Stone and G. M. Whitesides, *Science*, 2002, 295, 5555, 647–651.
2. A. D. Stroock, S. K. Dertinger, G. M. Whitesides and A. Ajdari, *Analytical Chemistry* , 2002, 74, 20, 5306–5312.
3. C.H. Lin, G.B. Lee, L.M. Fu, B.H. Hwey, 2004 *J Microelectromechanical Systems* 13, 923-932
4. H. Wang, P. Iovenitti, E. Harvey and S. Masood, *Journal of Micromechanics and Microengineering*, 2003, 13 801–808.
5. P. Sundararajan , J. Kirtland , D. Koch and A. Stroock, "Separation by diffusive irreversibility in a chaotic Stokes flow in a microchannel", *American Physical Society*, Division of Fluid Dynamics, November 23-25, 2008.
6. A. Wolff, I. R. Perch-Nielsen, U. D. Larsen, P. Friis, G. Goranovic, C. R. Poulsen, J. P. Kutter, and P. Telleman, "Integrating advanced functionality in a

microfabricated high-throughput fluorescent-activated cell sorter", *Lab on a Chip*, 2003, 3, 22-27.
7. M.M. Wang, E. Tu, D.E. Raymond, J.M. Yang, H. Zhang, N. Hagen, B. Dees, E.M. Mercer, A.H. Forster, I. Kariv, P.J. Marchand, and W.F. Butler, "Microfluidic sorting of mammalian cells by optical force switching" *Nature Biotechnology*, 2004, 23, 83-87.
8. P. Yager, T. Edwards, E. Fu. K. Helton, K. Nelson, M.R. Tam, and B.H. Weigl, "Microfluidic diagnostic technologies for global public health", *Nature*, 2006, 442, 412-418.
9. J.P. Golden, J.S. Kim, J.S. Erickson, L.R. Hilliard, P.B. Howell, G.P. Anderson, M. Nasir and F.S. Ligler "Multi-wavelength microflow cytometer using groove-generated sheath flow" *Lab on a Chip*, 2009, 9, 1942-1950.
10. S.C. Jacobson, J.M. Ramsey, *Analytical Chemistry*, 1997, 69:3212–3217
11. G. Blankenstein, U.D. Larsen, *Biosensor & Bioelectronics*, 1998, 13:427–438
12. N. Hashemi, P.B. Howell, Jr., J.S. Erickson, J.P. Golden, and F.S. Ligler, *Lab on a Chip*, 2010, 10, 1952-1959.
13. N. Hashemi, H. Dankowicz, and M.R. Paul, "The nonlinear dynamics of tapping mode atomic force microscopy with capillary force interactions", *Journal of Applied Physics*, 2008, 103, 093512.
14. M.J. Fuerstman, P. Garstecki, and G. M.Whitesides, "Coding/Decoding and Reversibility of Droplet Trains in Microfluidic Networks" *Science*, 2007, 315 (5813), 828.
15. P. Paik, V. K. Pamula and R. B. Fair, "Rapid droplet mixers for digital microfluidic systems", *Lab on a Chip*, 2003, 3, 253-259
16. G. I. Taylor, National Committee for Fluid Mechanics Films (Education Development Center, Newton, MA, 1966.
17. G. Düring, D. Bartolo, and J. Kurchan, "Irreversibility and self-organization in hydrodynamic echo experiments" *Physical Review E*, 2009, 79, 030101 (R).
18. C. Hansen, K. Leung, P. Mousavi , "Chipping in to Microfluidics" Physics World, 2007
19. G. Leal, "Laminar Flow and Convective Transport Processes", Butterworth-Heinemann, 1992
20. J.P. Heller, "An Unmixing Demonstration", *American Journal of Physics*, 28, 348-353, 1960.
21. H.Y. Tan, W.K. Loke, Y.T. Tan and N.T. Nguyen, Lab on a Chip, 2008, 8, 885 – 891.
22. P.B. Howell, D.R. Mott, F.S. Ligler, J.P. Golden, C.R. Kaplan, and E.S. Oran "A combinatorial approach to microfluidic mixing" *Journal of Micromechanics and Microengineering*, 2008, 18, 115019-11501.
23. P.B. Howell, D.R. Mott, S. Fertig, C.R. Kaplan, J.P. Golden, E.S. Oran and F.S. Ligler, "A microfluidic mixer with grooves placed on the top and bottom of the channel", *Lab on a Chip*, 2005, 5, 524-530.
24. P.B. Howell, J.P. Golden, L.R. Hilliard, J.S. Erickson, D.R. Mott and F.S. Ligler, "Two simple and rugged designs for creating microfluidic sheath flow" *Lab on a Chip*, 2008, 8, 1097-1103.
25. J.S. Kim, G.P. Anderson, J.S. Erickson, J.P. Golden, M. Nasir, and F.S. Ligler "Multiplexed detection of bacteria and toxins using a microflow cytometer", *Analytical Chemistry*, 2009, 81, 5426-5432.
26. D.C. Duffy, J.C. McDonald, O.J.A. Schueller, and G.M. Whitesides, "Rapid Prototyping of Microfluidic Systems in Poly(dimethylsiloxane)", *Analytical Chemistry*, 1998, 70 (23), 4974-4984.
27. T.M. Squires, and S.R. Quake, "Microfluidics: Fluid physics at the nanoliter scale", *Reviews of Modern Physics*, 2005, 77, 977-1026.
28. K.J. Morton, K. Loutherback, D.W. Inglis, O.K. Tsui, J.C. Sturm, S.Y. Chou, and R.H. Austin, "Crossing microfluidic streamlines to lyse, label and wash cells", *Lab on a Chip*, 2008, 8, 1448-1453.
29. M.T. McBride, D. Masquelier, B.J. Hindson, A.J Makarewicz, S. Brown, K. Burris, T. Metz, R.G. Langlois, K.W Tsang, R. Bryan, D.A. Anderson, K.S. Venkateswaran, F.P. Milanovich, and B.W Colston Jr., "Autonomous Detection of Aerosolized *Bacillus anthracis* and *Yersinia pestis*", *Analytical Chemistry*, 2003, 75, 5293-5299.
30. S. Riethdorf, H. Wikman, and K. Pantel, "Review: Biological relevance of disseminated tumor cells in cancer patients", *International Journal of Cancer*, 2008, 123(9), 1991-2006.